

7-1-2007

# Reliability of Concrete Masonry Unit Walls Subjected to Explosive Loads

Christopher D. Eamon

Mississippi State University, Starkville, MS, christopher.eamon@wayne.edu

---

## Recommended Citation

Eamon, C. D. (2007). "Reliability of concrete masonry unit walls subjected to explosive loads." *Journal of Structural Engineering*, 133(7), 935-944, doi: 10.1061/(ASCE)0733-9445(2007)133:7(935)  
Available at: [https://digitalcommons.wayne.edu/ce\\_eng\\_frp/6](https://digitalcommons.wayne.edu/ce_eng_frp/6)

This Article is brought to you for free and open access by the Civil and Environmental Engineering at DigitalCommons@WayneState. It has been accepted for inclusion in Civil and Environmental Engineering Faculty Research Publications by an authorized administrator of DigitalCommons@WayneState.

RELIABILITY OF CONCRETE MASONRY UNIT WALLS SUBJECTED TO  
EXPLOSIVE LOADS

Christopher D. Eamon, M.ASCE<sup>1</sup>

Subject Headings: Reliability, Blast Loads, Concrete Masonry, Walls, Explosions, Concrete structures; Concrete blocks

ABSTRACT

This study discusses the development of a procedure that can be used to assess the reliability of concrete masonry unit infill walls subjected to personnel-delivered blast loads. Consideration is given to maintain reasonable computational effort for both the structural analysis and reliability models. Blast load and wall resistance models are developed based on experimental and analytical data, and resistance is evaluated with a large strain, large displacement transient dynamic finite element analysis. A sensitivity analysis is conducted to identify significant random variables and a reliability analysis conducted with a feasible level of computational effort. Reliability indices are estimated for two wall types and three design blast load levels in terms of wall failure as well as occupant injury, over various load frequency-of-occurrence times.

-----  
<sup>1</sup>Associate Professor, Department of Civil Engineering, Mississippi State University, Starkville, MS 39762. email: eamon@engr.msstate.edu

## INTRODUCTION

Since 9/11, many government buildings have been secured from vehicular-delivered threats with road closings and barricades that enforce vehicular stand-off distances. Numerous studies have been conducted on various hardening techniques, and some limited design guidance has been developed to protect against these large blast loads (Volkman 1990; Hamad, 1993; Corley et al. 1993; Dharaneepathy et al. 1995; Ettouney et al. 1996; Longinow et al. 1996; Otani et al. 1997; Crawford et al. 1997; Murray 1997; Barakat et al. 1999; Krauthammer et al. 1997; Rose et al. 1997, 1998; Zehrt et al. 1998; Hinman 1998; ACI-ASCE 1998).

A remaining concern is the damage caused from smaller, personnel-delivered threats that may be delivered to the building by a terrorist carrying an explosive charge on his person. A common existing façade for many target-prone government buildings is made of non-load bearing, unreinforced concrete masonry unit (CMU) walls infilled between building floors (Dennis et al. 2002). From a life-safety point of view, the most critical concern from a low-magnitude, personnel-delivered blast load (i.e. blasts below a level which would cause building collapse) is when debris from the facade is projected into the building and strikes occupants. Recognizing this concern, the U.S. Army Corps of Engineers (USACE) recently conducted a series of experimental tests of this construction type subjected to various blast loads to gather response data and to aid in assessing the extent of the problem (Dennis et al. 2002). These results were subsequently used to develop numerical models for future studies of façade performance evaluation and retrofit options (Eamon et al. 2004).

Due to the uncertainties that exist in structural resistance as well as load effects, safety is measured probabilistically, typically with the reliability index. However, other than an

exploratory study done by Low (2001; 2002), who estimated the reliability of reinforced concrete slabs under blast loads using simple single degree of freedom models, and later by Stewart et al. (2006), who considered the probabilistic response of glazing systems, there is no readily available information evaluating the reliability of civil engineering structures exposed to blast loads.

The objective of this study is to fill this gap for a type of structure often exposed to blast loads and develop a procedure that can be used to estimate the structural reliability of unreinforced CMU infill walls subjected to explosive loads. Consideration is given to maintain a feasible level of computational effort with regard to both the structural analysis as well as the reliability models. In doing so, this study investigates the safety of exterior unreinforced CMU infill walls subjected to 3 personnel-delivered blast levels. Reliability is given in terms of wall failure as well as occupant injury criteria.

## FINITE ELEMENT MODEL

As unreinforced CMU walls often fragment under blast loads, a rigorous description of wall behavior requires a highly nonlinear, transient dynamic, large strain, large displacement approach that allows arbitrary element contact and separation, as well as an accurate prediction of both wall failure and resulting debris velocity. Eamon et al. (2004) developed a numerical model that provided good comparison to the existing experimental data, in terms of both wall failure and debris velocity. The models were solved with a readily available commercial code DYNA3D (LLNL 1999), and are used for this study. Full details of the models and comparisons to the experimental results are given elsewhere (Eamon et al. 2004). A brief summary of the

structural model is presented here, while a description of the blast loads is provided in the section *Load Model*.

Two wall types are considered: fully-grouted, in which the cores of the CMUs are filled with grout, and ungrouted, in which the cores are left hollow. The walls are composed of fifteen rows of standard 8x8x16 nominal CMUs (wall height approximately 3.3 m), producing a wall height/thickness aspect ratio of 15:1. Based on high-speed video studies of the 6m (15 block) long test walls, the experimental data indicated that walls behaved in a one-way fashion, with no significant variation in deformation along wall length (i.e. in the horizontal direction). Walls were thus modeled similarly to a plane-strain model in which length of the wall is represented by a unit-length stack of CMU blocks, as shown in Figure 1. Full details of the experimental results are given elsewhere (Dennis et al. 2002; Eamon et al. 2004). In general, however, the test walls had the geometry described above, were constrained at the top and bottom with side edges free (representing an in-fill wall between building columns) and exposed to a blast load with parameters described later.

As the model is concerned with the global failure and fragmentation behavior of the walls rather than the stress gradients within the CMU blocks, each of the fully-grouted CMUs was modeled with two hexahedral elements to minimize computational effort. It was found that further refinement in mesh density did not significantly improve global results. This suggests that CMU interconnectivity and contact parameters along joint lines, rather than individual block deformations, govern global wall behavior. UngROUTED CMUs were modeled with a minimal number of elements needed to define the geometry.

The idealized ungrouted 8x8x16 CMUs are modeled with dimensions of 203 mm x 203 mm x 406 mm with equivalent density of 1550 kg/m<sup>3</sup>. The mortar itself (type M) is modeled as a

zero-thickness contact surface, which initially rigidly links adjoining blocks together. When a specified failure criterion is reached, based on a combination of normal and in-plane shear stresses, the slide surface releases the nodal constraints. The coefficients of friction were taken as 0.50 between CMU surfaces. The CMU material law was taken as a Mohr-Coulomb failure surface with a Tresca limit. In this model, cohesion is taken as zero and friction angle is indirectly defined by an experimentally found principal pressure-shear stress relationship. Based on experimental data, the pressure-volume relationship for the CMUs is described with a simple equation of state that describes pressure as a linear function of volumetric strain (Dennis 2000). The model also assumes strengthening under higher (compressive) strain rates, which is based on enhancements to compressive strength as reported in DOE/TIC 11268 (1992). Material properties were taken from the experimental data and existing literature (Eamon et al. 2004).

The CMUs, at the top and bottom of the interface between the wall and its confining frame (the floors of the building), were paired with a more refined mesh and material model that allows element deactivation once a specified failure pressure is reached. It was found that this formulation was essential to properly capture the material crushing that occurs at the top and bottom CMUs. A special slide surface is specified between these CMU surfaces and the frame, that adapts to the new material boundary as failed elements are removed. The building floors holding the top and bottom of the wall in place were modeled as rigid. Here the façade is much less stiff than a typical building frame, and at the load levels considered for this study, the façade will fail before any significant response is realized by the building structure. With a base set of material parameters, this model correctly matched each of the 15 available experimental wall test results in terms of failure/survival as well as produced reliable results for debris velocity (Eamon et al. 2004).

## LOAD MODEL

For this study, data from 43 experimental blast load tests on CMU walls recently conducted by USACE were made available. These are the tests that were modeled with the FEA procedure described above. The test loads were chosen by USACE with varying standoff distances and charge weights, to represent an expected range of explosive threat levels. Due to security concerns, detailed load data, and in particular, specific charge weights and standoff distances, are not available for public release. However, the time-history of the resulting blast pressures and in particular the impulse delivered to the walls were statistically analyzed, and quantitative results are presented below. Based on the impulse levels delivered to the walls and resulting wall behavior, three general blast pressure levels were specified: low, moderate, and high. From an examination of wall surface pressures taken from the experimental results (Dennis et al. 2002; Eamon et al. 2004), a time-varying, uniform pressure over the entire wall surface is applied for analysis.

Although expressions for the shape of load curve have been developed and are typically exponential in form (Beshara 1992), these highly idealized curves were found to have an insufficient number of control parameters to match the actual experimental data well. Therefore, special curves were developed for this study. Load curves are idealized by 4 piecewise linear functions, two positive and two negative, as shown in Figures 2 and 3. This form matched the shape of the actual blast curves well and, more importantly, could exactly satisfy the values and interaction of the load random variables. Seven random variables (RVs) are used to describe the load curve, as given in Tables 1 and 2, and shown in bold in Figure 3. These include: the primary positive impulse ( $I_{p1}$ ); the secondary positive impulse ( $I_{p2}$ ); the negative impulse ( $I_n$ );

the zero pressure time (zt); the peak pressure (pp); the low pressure (lp); and the low pressure time (lt). As shown in Figure 3, for each load case, the points (t, m) and (e,0) are found such that the RV values are satisfied. RV variation originates from three primary sources: expected standoff distance, charge weight, and the variation in the explosive material itself. The resulting range of considered blast pressures were to represent current, reasonably expected threat levels. Currently, there is insufficient test information to well-define the RV distributions. Thus, they are taken as normally distributed. As more information becomes available through additional experimental or field findings, the load model can be updated.

## RESISTANCE MODEL

Numerous experimental and numerical studies have examined concrete wall response to blast loads. Some of these contributions include Klaus (1985); Beshara et al. (1991, 1993); Kraus et al. (1994); Krauthammer et al. (1994, 1997); Murray (1997); Zehrt et al. (1998); Lok et al. (1999); Mays et al. (1999); and Baylot et al. (2005), among others. However, the research of Dennis et al. (2002) and Eamon et al. (2004) is particularly relevant here, which concerns the specific blast loads and CMU walls considered in this study. Previous research has shown that numerous resistance parameters may affect unreinforced CMU wall behavior under blast loads. Some of these include wall height/thickness ratio, wall mass, mortar joint strength, block strength, and friction between contacting block surfaces and between the block-building frame contact surface once fracture occurs. For this study, mass and wall aspect ratio are held constant as per the experimental data made available. Eamon et al. (2004) conducted a deterministic sensitivity analysis to identify the importance of the remaining resistance parameters.

Depending on a parameter's level of variance, the set of parameters that are important in a deterministic analysis are not necessarily identical to those in a reliability analysis. To this end, a sensitivity analysis was conducted to identify the potential random variables which most influence wall response. The analysis was conducted for a variety of parameters that potentially could be taken as RVs for the particular CMU walls considered in this study: mortar joint modulus of rupture (Mortar MOR); contact friction between CMU surfaces (CMU-CMU  $\mu$ ); contact friction between the CMU and top and bottom building floors (CMU-frame  $\mu$  top) and (CMU-frame  $\mu$  bot); and for the CMUs, Poisson ratio; compressive strength ( $f'_c$ ); tensile strength ( $f_t$ ); modulus of elasticity (E); shear modulus (G); bulk modulus (K); and strain rate strengthening. For initial RV selection, the sensitivity of maximum debris velocity  $v$  (as a measure of wall failure propensity as well as occupant injury) to variable  $x_i$  was numerically estimated with:  $(\partial v / \partial x_i) \sigma_i$ , where  $\sigma_i$  is the standard deviation of the RV (Melchers 2002). To allow the consistent comparison of random variable sensitivities with different means, standard deviation is non-dimensionalized by dividing by mean value. Normalized results are presented in Figure 4. Based on the sensitivity results, a total of 31 parameters are identified for use as resistance RVs as shown in Table 3: one for each of the mortar joints MOR (mj 1 - mj15) and friction coefficients ( $\mu_j$  1 -  $\mu_j$ 14) between each CMU and one each for friction coefficients between the CMU blocks at the top ( $\mu_t$ ) and bottom ( $\mu_b$ ) of the wall and building frame. Statistical data are taken from the existing experimental data (Eamon et al. 2004; NCMA 1994; Dennis 2000; Rabbat et al. 1985; Mirza et al. 1979; Klink 1985; Lew et al. 1978). All RV distributions are normal. One interesting result uncovered in the numerical modeling by Eamon et al. (2004) was that using a constant value for mortar flexural strength for both grouted and ungrouted walls best predicted blast response in both cases. This is in contrast to the static tests,

which have shown large increases in MOR for grouted walls (see, for example, Hamid et al. 1988). In this study, the more conservative blast load parameters are used in which no increase in mortar MOR is given to grouted walls.

No data are available on the resistance RV correlations. To determine the effects of resistance RV correlation on reliability for the entire 6m (15 block) wide by 15 block high wall considering all of the RVs above would require a minimum of approximately 930 full-wall finite element runs. As a single run of a full-wall finite element model requires approximately 20 CPU-hours using the computational resources available, the estimated computational effort required (approximately 22,000 CPU hours) to fully investigate resistance RV correlation is infeasible. However, reasonable bounds of reliability considering correlation can be made by studying the behavior of the wall structural system.

As noted previously, the walls displayed little to no variation in displacement along their length, which allowed for the accurate use of the quasi plane-strain finite element model (Eamon et al. 2004). Based on this uniformity of behavior, the blocks within each row are conceptually grouped together and taken as a ‘component’ in the wall system. Within each row component, the elimination of any single block has minimal effect on total row capacity, and does not necessitate failure of the entire row. Thus, each row of blocks behaves similarly to a parallel structural system. The fifteen stacked row components, in contrast, behave similarly to a series structural system, whereby the removal of a single row of blocks would result in wall collapse. The entire wall system is then conceptually modeled as a series system of rows, which in turn are parallel subsystems of the individual CMU blocks. Note this simple system model is not used to directly compute reliability, but only to aid in determining an appropriate choice for resistance RV correlation. Based on this model, the following assumptions are used:

1. A parameter value along the wall length does not change. That is, within a particular row of CMUs, friction and strength properties of one block are identical to the adjacent block. Therefore, the model assumes full correlation for a particular CMU property (strength or friction) within a given row of blocks. This corresponds to the blast test observations of uniform (length-wise) wall deformation and allows for efficient use of the existing numerical model. Assuming each row approximates the behavior of a parallel sub-system, the fully-correlated case is conservative with respect to reliability index, as this represents the lower bound of reliability in a parallel system.

2. Row component resistance RVs are statistically independent. Assuming the wall approximates a series system in the vertical direction (failure of a row subsystem with the wall results in failure of the wall), this assumption is conservative with respect to reliability index, as the statistically independent and thus uncorrelated case represents the lower bound of reliability in a series system. This assumption was verified numerically using the unit-length finite element model, which yielded a slightly lower capacity considering uncorrelated RVs as compared to the fully-correlated case.

## RELIABILITY ANALYSIS

Two measures of failure are considered: 1) the structural failure of wall, defined as collapse; and 2) failure due to unacceptably high debris velocity, which may cause serious injury to building occupants. Ideally, failure probability is calculated by integrating the joint probability density function of the limit state over the failure region, but this is typically infeasible. Although

simulation methods such as Monte Carlo are the potentially most accurate alternative, results of initial reliability studies of this problem have indicated that this approach, even when applying variance reduction techniques (such as importance sampling or adaptive importance sampling) are prohibitively computationally expensive, costing many hundreds to several thousands of simulations (i.e. runs of the FEA model) to adequately capture failure probability. Thus, to maintain computational feasibility, reliability index ( $\beta$ ) will be calculated as a surrogate for failure probability ( $P_f$ ).

In this study, as the limit state is an implicit function of the RVs as evaluated with the finite element method, a numerical approach is required to evaluate reliability index. Here the generalized first order reliability (FOR) method can be used (Melchers 2002), where the limit state  $g$  is linearized and non-normal distributions are converted to equivalent normal distributions at the most probable point of failure (MPP), which can be found through a standard iterative optimization algorithm, such as that developed by Rackwitz and Fiessler (1978). This procedure requires approximately  $n+1$  calls to the FEA code per iteration,  $n$  being the number of RVs in the problem. The number of iterations required for convergence is a function of problem nonlinearity and non-normality of RV distributions, but often 3 or 4 iterations are sufficient for reasonable accuracy. Thus, a minimum of approximately  $3(n+1)$  finite element analyses would be required.

A drawback of this numerical approach to evaluate  $\beta$  is that actual statistical parameters for load and resistance are not directly generated and remain unknown. An alternative solution, which may be more conceptually informative with regard to load and resistance, is to develop single-RV statistical measures of load and resistance by expressing the 31 resistance RVs as an equivalent global resistance RV  $R$  and the 7 load RVs as an equivalent global load RV  $Q$ . If this

information is known, an explicit limit state can be developed and  $\beta$  can be quickly calculated using any appropriate method such as FOR. This is the approach taken in this study.

It was observed that load impulse is by far the primary determinant of wall failure or survival, as well as debris velocity (Eamon 2002). Therefore, the limit state function  $g = R - Q$ , will be formed in terms of impulse. Here load effect  $Q$  must be in terms of impulse imparted to the wall while resistance  $R$  must be in terms of impulse that the wall can resist. The next step is to generate global statistical parameters for  $Q$  and  $R$ .

### Reliability Based on Wall Failure

Statistical parameters for impulse load  $Q$  are generated by Monte Carlo Simulation (MCS). Correlations were accounted for by directly including the relationships in Table 1 in the simulation. From these data sets an equal number of load curves are constructed, while eliminating the few physically invalid curves that contained reverse-sign RV values. Mean load curves are presented in Figure 5 for low, moderate, and high pressure cases. Each of the resulting load curves is then integrated to find its maximum impulse. From this resulting data set, the mean value and coefficient of variation (COV) of  $Q$  can be calculated. Based on 1000 MCS results, the blast load statistical parameters are:

- For low pressure blasts, mean  $Q = 217$  KPa-msec and  $COV = 0.17$
- For moderate pressure blasts, mean  $Q = 479$  KPa-msec and  $COV = 0.09$
- For high pressure blasts, mean  $Q = 607$  KPa-msec and  $COV = 0.08$

Notice that COV decreases as blast pressure increases. This occurs for several reasons. First, considering blast material variability, standard deviation is approximately the same for all charge weights, resulting in a lower normalized variation (COV) as charge weight becomes larger. A second reason for this is there is a practical upper limit for personally-transportable charge weight sizes, further limiting variance for larger charges. Finally, sensitivity of wall blast pressure to stand off distance is reduced for larger charges (keeping the range of stand off distance approximately constant for all charge weights).

The load data for each of the three impulse curves were fit to normal, lognormal, and extreme type I distributions. The Kolmogorov-Smirnov (KS) test (Ang and Tang 1975) was used to measure goodness of fit. Both the entire distribution as well as the upper tails were considered. In the latter case, the upper 5% of the data were used. Considering the entire distributions, the low and high pressure impulse data best fit a lognormal distribution ( $D=0.039$  and  $D=0.16$ , respectively, where  $D$  is the maximum difference between CDF values at any point of the actual data and the fitted distribution type), while the moderate pressure impulse data best fit a normal distribution ( $D=0.019$ ). Considering the upper tail, the low pressure impulse data best fit lognormal ( $D=0.039$ ), with normal the next-best fit ( $D=0.051$ ). The moderate pressure impulse curve also best fit normal ( $D=0.0027$ ), while the high pressure curve best fit extreme type I ( $D=0.011$ ), with the next-best fit being normal ( $D=0.015$ ). The sensitivity of reliability with regard to load distribution type is explored below. Probability density functions of impulse load data are shown in Figure 6, while cumulative density functions are given in Figure 7.

Mean wall resistance  $R$  is linearly approximated at the failure point by first setting all load and resistance RVs at their mean values. Load is then increased until wall failure by incrementing (by linear interpolation) the shape of pressure curve from the mean low to the mean

moderate blast pressure cases (all walls failed between these two blast pressures). Because the problem is transient dynamic and not static, each load increment requires a separate analysis with a separate (incremented) load curve. At the precise event of failure, load effect equals resistance. Thus, the smallest incremented load curve that resulted in wall failure is also equal to the resistance value of the wall (within 1% error, the increment value). This load curve is then integrated to find the maximum mean impulse  $Q = R$  imparted to (and thus resisted by) the wall. Mean load curves resisted are given in Figure 8.

To calculate reliability index, variance of  $R$  is also needed. Resistance variance is estimated with a  $2n+1$  point estimation method (Rosenblueth 1981; Nowak and Collins 2000). This process requires  $2n$  evaluations (or 62 per wall), with each simulation conducted with a perturbed  $RV$  value. For each simulation, load is increased until failure by incrementing the shape of blast curve as described above, and this load (resistance) value is recorded. The COV of the function can then be estimated as:

$$COV_Y = \sqrt{\left[ \prod_{i=1}^n (1 + V_{y_i}^2) \right] - 1} \quad (1)$$

where

$$V_{y_i} = \frac{y_i^+ - y_i^-}{y_i^+ + y_i^-} \quad (2)$$

Here  $y_i^+$  refers to the resistance result with  $RV$   $i$  perturbed up one standard deviation, while  $y_i^-$  refers to the resistance result with  $RV$   $i$  perturbed down one standard deviation, with all other  $RV$ s kept at their mean values. The results are:

- For grouted walls, mean  $R = 356$  KPa-msec and  $COV = 0.18$
- for ungrouted walls, mean  $R = 219$  KPa-msec and  $COV = 0.21$

Notice that the COV for grouted walls is slightly less than that for ungrouted walls. The reason for this is that the grout adds substantial mass to the wall. Mass has a significant effect on wall performance, but as mass itself is an approximately deterministic quantity (variation in CMU volume and grout mass is very small, and the effect on  $\beta$  was found to be small relative to the other RVs considered, so mass was not included as RV), the sensitivity of  $\beta$  to the remaining RVs decreases when wall mass is increased. Thus, adding grout has an overall effect of reducing variance with respect to failure behavior under the blast loads considered.

Although computationally efficient, a drawback of this approximate method used to compute resistance variance is that no information can be gathered regarding distribution type. Thus, resistance is assumed to be normal, a distribution which is expected to be approached for a response which is a function of multiple normal RVs.

It is important to note that in this approach, even though each of the many load and resistance RVs are not explicitly expressed in the limit state, they are implicitly captured in the final results, as changing any of the RV values will (potentially) affect the final values calculated for Q or R. Further, wall resistance values are based on the specific blast pressure, wall geometry and boundary conditions, and material properties used in this study. Resistance results would not be valid for other wall types or impulse values generated from other shapes of pressure curves with different RV relationships, and would have to be recalculated with the FEA model in these cases.

Note that the procedure described above does not yet account for load frequency of occurrence, which may dramatically affect lifetime reliability. Expected rate of return, however, varies tremendously with the specific building considered, and is difficult to accurately quantify.

In this case, rather than assume a single load frequency value for all buildings, a more reasonable approach may be to provide results from a series of load frequencies from which a designer can choose as appropriate for a particular building. Wall reliability index  $\beta_w$  considering blast occurrence probability can be approximated as:

$$\beta_w = -\Phi^{-1}\left(\left(P_{fw} P_e\right)\right) \quad (3)$$

where

$\Phi$  = Cumulative distribution function for a standard normal random variable

$P_e$  = Probability of occurrence of the blast load event

$P_{fw} \approx \Phi(-\beta_1)$ , the probably of failure of the wall given that a blast load event has occurred

$\beta_1$  = Reliability index of wall that is exposed to a blast load with  $P_e = 1.0$

Thus, if  $P_e = 1.0$ , there is a 100% probability that the structure will experience a blast load once in its design lifetime (for example, once in 50 to 75 years) with the mean impulse load value as given. Results considering various probabilities of load occurrence ( $P_e = 1.0, 0.10, 0.01, 0.001$ , and  $0.0001$ ) are presented in Table 4, where reliability indices are calculated considering a normal, lognormal, and extreme type I load distribution. In the tables, the reliability index computed with the best-fit load distribution is highlighted.

For  $P_e = 1.0$ , the results indicate that the CMU walls considered in this study have a high failure probability to a personnel blast of a moderate and high severity, and are unreliable for even a low level blast. This result is expected based on the previous experimental and numerical work (Dennis et al. 2002; Eamon et al. 2004.) Also expected is that normally distributed loads typically result in the highest reliabilities, where extreme distributions typically result in the lowest. The influence of load distribution becomes more significant as failure probability

increases, and it thus is most influential on ungrouted walls as well as higher load magnitudes. As the probability of occurrence is decreased, the differences in reliability index due to the effects of load distribution, wall type (grouted walls being more reliable due to increased wall mass and mortar joint strength), and blast load pressure seen in Table 4 quickly disappear. This trend is particularly true for the negative indices, for which  $P_e$  dominates failure probability rather than load effect. Negative reliability indices indicate that failure probability is greater than 50%, while positive values indicate that failure probability is less than 50%. An approximate indication of failure probability can be determined by the transformation:  $P_f = \Phi(-\beta)$ , where  $\Phi$  is the standard normal cumulative distribution function. In Table 4, all  $P_e = 1.0$  wall reliability indices equal to about -2 or less are completely governed (practically) by occurrence probability. This can be seen further in the table, where the lower bound of  $\beta$  is 1.28 for  $P_e = P_f = 0.10$ , 2.33 for  $P_e = 0.01$ , 3.09 for  $P_e = 0.001$ , and 3.72 for  $P_e = 0.0001$ . It appears that, for the walls and blast loads considered, load occurrence probabilities between 0.001 and 0.0001 generally produce reliability indices with adequate levels of safety, as compared to typical Load and Resistance Factor Design code results, which typically have strength limit state reliability indices between 3-4 assuming a 50 to 75 year design lifetime.

Recall failure is defined as wall collapse. That is, reliability is calculated for the state just when the wall topples, but with essentially zero debris velocity. Although this constitutes a failure from a structural standpoint, this metric is very conservative from a human injury perspective. Therefore, an additional criterion is considered based on expected occupant injury.

#### Reliability Based on Critical Debris Velocity

A number of experimental studies sponsored by the Department of Defense have analyzed personal injury severity from blunt debris strikes (Clare et al. 1975; Cooper et al. 1986; Bir et al. 2004). These studies have approached the problem with different projectile and target characteristics as well as varying injury measurement techniques. To date, no study has accounted for all of the relevant parameters, as many factors affect results, including both projectile parameters (impulse delivered to target, contact area and shape, projectile compliance) as well as target factors (age, weight, sex, health, impact location, medical care available) (Widder 2000). The overall problem is complex. However, general results, in terms of critical projectile and target parameters, have been consistent. Injury criteria for this study is based on the experimental work of Clare et al. (1975), who generated injury curves resulting from blunt trauma as a function of the most critical projectile and target parameters. Based on this data, ‘severe’ injury (taken as unacceptable, where some deaths are expected) is modeled with the following empirical equation:

$$\ln(WD) = 1.03 \ln(MV^2) - 7.94 \quad (4)$$

where

W = weight of target (kg)

D = diameter of projectile (cm)

M = mass of projectile (g)

V = velocity of projectile (m/s)

Based on an typical individual (W=73kg) and CMU debris properties, using equation (4), failure is defined when debris velocity (V) reaches the following critical values: for grouted

walls,  $V=11.5$  m/s, while for ungrouted walls,  $V = 15.5$  m/s. Recall that, as indicated in the experimental and analytical data discussed above, the CMU walls tend to fail at the mortar joints. Therefore, projectile properties (mass, dimensions) are based on a typical intact CMU block. Although it is conceivable that multiple blocks might impact a single target, due to the potential of various obstacles in the trajectory path as well as a lack of experimental data on the effects of multiple-object impact, this simple first strike injury criterion is used for this study.

For the reliability analysis, the limit state remains in terms of impulse, but now resistance must be reformulated in terms of wall resistance to critical debris velocity rather than wall failure. To determine the statistical parameters for resistance, the procedure used above for wall failure is duplicated, but now rather than finding the load curve increment that results in wall failure, the load curve increment that causes the critical debris velocity is considered. Results of the analysis for critical velocity causing unacceptable occupant injury are:

- For grouted walls, mean  $R = 455$  KPa-msec and  $COV = 0.095$
- For ungrouted walls: mean  $R = 328$  KPa-msec and  $COV= 0.11$

Mean load curves resisted are shown in Figure 8. By observing the decrease in resistance COV, it is clear that debris velocity is less sensitive to variations in resistance RVs than wall failure. This finding is expected based on the existing experimental and (deterministic) analytical results, which found that for a given blast pressure, once the wall fails, debris velocity shows no significant dependence on wall failure mode (what mortar line cracked first, or whether top or bottom of wall slid from supports, etc.) (Eamon et al. 2004). This trend is also evident in the simple closed-form analytical equations used to roughly estimate debris velocity, which express

wall velocity as a function of load impulse and wall mass, but not failure mode (Dennis 2000). From a safety standpoint, this is of course fortunate as lower variance results in higher reliability indices.

Reliability index is again calculated for the load distribution types and occurrence probabilities considered earlier. Results are shown in Table 5. By comparing these values to those in Table 4, it is clear that significant improvement has been realized for  $P_e = 1.0$  results, particularly for the low pressure blast. For moderate and high pressure results, as with the wall failure criterion, reliability becomes dominated by probability of event occurrence rather than wall resistance capacity. For  $P_e = 0.10$  and less, reliability results for moderate and high pressures are not significantly different whether wall failure or debris velocity are considered.

## CONCLUSIONS

This study developed a procedure to examine the reliability of CMU infill walls subjected to personnel-delivered blast loads. The process and results are meant to be used as a tool for initial assessment of the reliability of CMU walls with reasonable computational effort. This research generated small personnel-delivered blast load statistics from experimental data, and resistance statistics from a large strain, large displacement transient dynamic finite element analysis. A sensitivity analysis was conducted to identify significant random variables and a reliability analysis was conducted considering several load distribution types and probabilities of occurrence. Reliability indices were estimated for wall failure as well as occupant injury. Based on the results, several conclusions can be drawn from this study. The following conclusions are limited to the specific CMU wall characteristics (i.e. with regard to geometry, construction, and materials) and blast loads considered in this study.

- With wall geometry, materials, and boundary conditions held constant, the most influential random variables that affect wall resistance are mortar joint strength and contact surface friction. For load, the most critical parameter is peak impulse. Both positive and negative pressure areas on the blast time-history affect wall response and should be included.
- Load event occurrence has a significant effect on failure probability, and governs reliability for moderate and high blast pressures when  $P_e$  is approximately 0.10 and less. Load event occurrence values between 0.001 and 0.0001 appear to result in walls with reliabilities comparable to those based on other common design loads, while a blast load event occurrence probability of 1.0 generally results in walls with low reliability.
- Load random variable distribution type has a significant effect on results with  $P_e = 1.0$ , with normally-distributed loads generally more safe than lognormal and extreme type I. For the critical velocity criteria, at  $P_e = 0.10$  and less, only low blast loads are practically affected by load distribution, while for moderate and high pressure blasts distribution type is insignificant. For the wall failure criteria, at  $P_e = 0.10$  and less, load distribution is insignificant.
- For all load event occurrence values, fully-grouted walls are more safe than ungrouted walls at low pressure loads, with differences in reliability index decreasing as  $P_e$  decreases. Considering the wall failure criteria, for both moderate and high pressure loads, wall type is insignificant at  $P_e = 0.10$  or less. Considering critical velocity, wall type is insignificant for high pressure loads at  $P_e = 0.10$  and less.
- Considering critical debris velocity, reliability indices for  $P_e = 1.0$  are significantly higher than for wall failure. However, for moderate and high pressure loads, for  $P_e = 0.10$  and

less, differences in reliability between wall failure and debris velocity criteria are generally small. Similar trends with respect to load event occurrence, wall type, load distribution, and load magnitude exist for reliability based on critical velocity as with wall failure.

For existing walls that are believed to be inadequate, various reinforcing options are possible and are discussed elsewhere (see, for example, some of the references identified in the introduction), though the effectiveness of these retrofits from a reliability perspective has not yet been investigated. Currently, there is a lack of research in this area. Most critical is the need to gather additional data to expand the development of the load model as well as to explore the reliability of additional wall characteristics, such as wall aspect ratios, construction types, and reinforcing options. More precise statistical data on wall resistance as well as resistance random variable correlation are needed as well. In order to quantify the safety risks involved in various design trade-offs, as well as to provide structural resistance to blast loads at a rational and consistent level, a significant amount of additional research effort in this area is called for.

## REFERENCES

- ACI-ASCE Committee, "Abstract of : Response of Concrete Building to Lateral Forces," *ACI Structural Journal*, Vol. 85, No. 4, 1988, pp. 472-478.
- Ang, A.H.S. and Tang, W.H. (1975). "Probability Concepts in Engineering and Planning Design." John Wiley & Sons, New York.
- Barakat, M.A. and Hetherington, J.G. "Architectural Approach to Reducing Blast Effects on Structures," *Proceedings of the Institution of Civil Engineers, Structures and Buildings*, Vol 134, No. 4, 1999, pp. 333-343
- Baylot, J. T., Woodson, S.C., O'Daniel, J.L., and Bullock, W. (2001). "Analysis and Retrofit of CMU Walls." *Proceedings of 2001 ASCE Structures Congress*, May 21-23, Washington, D.C.
- Baylot, J.T., Bullock, B., Woodson, S.C., and O'Daniel, J.L., "Blast Response of Lightly-Attached CMU Walls," *ASCE Journal of Structural Engineering*, v 131, n8, August 2005, pp. 1186-1193.
- Beshara, F.B.A., "Smearred Crack Analysis for Reinforced Concrete Structures under Blast-Type Lading," *Engineering Fracture Mechanics*, Vol. 45, No. 1, 1993, pp. 119-140.
- Beshara, F.B.A. and Viridi, K.S., "Time Integration Procedures for Finite Element Analysis of Blast-Resistant Reinforced Concrete Structures," *Computers and Structures*, Vol. 40, No. 5, 1991, pp. 1105-1123.
- Beshara, F.B.A. "Modeling of Blast Loading on Aboveground Structures I: General Phenomenology and External Blast." *Computers and Structures*, Vol 51, No 5, pp 585-596.
- Bir, C.A., Viano, D, and King, A. "Development of biomechanical response corridors of the

- thorax to blunt ballistic impacts.” *Journal of Biomechanics*, Jan 2004, Vol. 37, Issue 1, p 73-80.
- Clare, V.R., Lewis, J.H., Mickiewicz, A.P., and Sturdivan, L.M. “Blunt Trauma Data Correlation,” Technical Report no. EB-TR-75016. Aberdeen Proving Ground, MD: Edgewood Arsenal, May 1975: NTIS AD-A012 761.
- Cooper, G.J. and Maynard, R.L. “An Experimental Investigation of the Biokinetic Principles Governing Non-Penetrating Impact to the Chest and the Influence of the Rate of Body Wall Distortion Upon the Severity of Lung Injury.” *Proceedings of the IRCOBI European Impact Biomechanics Conference*, Zurich, Switzerland, 1986.
- Corley, W.G., Mlakar, P.F., Sozen, M.A., and Thornton, C.H. “The Oklahoma City Bombing: Summary and Recommendations for Multi-Hazard Mitigation.” *ASCE Journal of Performance of Constructed Facilities*, August 1998, pp. 100-112.
- Crawford, J.E., Malvar, J, Wesevich, J.W., Valancius, J., and Reynolds, A.D. “Retrofit of Reinforced Concrete Structures to Resist Blast Effects.” *ACI Structural Journal*, July-August 1997, pp. 371-377.
- Dennis, S.T. (2000). “Masonry Walls Subjected to Blast Loading, Technical Report SL-00-2000.” US Army Corps. of Engineers, Waterways Experiment Station.
- Dennis, S.T., Baylot, J.T., and Woodson, S.C. (2002). “Response of 1/4-Scale Concrete Masonry Unit (CMU) Walls to Blast.” *ASCE Journal of Engineering Mechanics*, Vol 128 No. 2, pp 134-142, 2002.
- Dharaneepathy, M.V., Rao, K., and Santhakumar, A.R. “Critical Distance for Blast-Resistant Design.” *Computers and Structures*, Vol. 54, No. 4, pp. 587-595, 1995.

- DOE/TIC 11268 (1992). "A manual for the prediction of blast and fragment loadings on structures." US Department of Energy.
- Eamon, C., Baylot, J.T, O'Daniel, J.L. "Finite Element Modeling of Concrete Masonry Unit Walls Subjected to Explosive Loads," ASCE Journal of Engineering Mechanics, Vol 130, No. 9, pp 1098-1106, 2004.
- Eamon, C.D. "Distributed Anti-Terrorist Environment: Finite Element Modeling of Concrete Masonry Unit Walls Subjected to Explosive Loads." Mississippi State University, Dept. of Civil Engineering. Report Submitted to US Army Corps of Engineers, Engineer Research and Development Center. February 2002.
- Etouney, M., Smilowitz, R., and Rittenhouse, T. "Blast Resistant Design of Commercial Buildings." ASCE Practice Periodical on Structural Design and Construction. Feb. 1996. pp. 31-39.
- Hamad, B.S. "Evaluation and Repair of War-Damaged Concrete Structures in Beirut." ACI Concrete International, March 1993, pp. 47-51.
- Hamid, A.A. and Drysdale, R.G. "Flexural Tensile Strength of Concrete Block Masonry." ASCE Journal of Structural Engineering, v114, n1, January, 1988, pp 50-66.
- Hinman, E., "Approach for Designing Civilian Structures Against Terrorist Attack," *Concrete and Blast effects*, by American Concrete Institute, SP-175, edited by Bounds, W., 1998, pp. 1-17.
- Klaus, M.H. "Response of a Panel Wall Subjected to Blast Loading," *Computers and Structures*, v 21, n 1-2, 1985, Nonlinear Finite Elem Anal and ADINA, Proc of the 5th ADINA Conf, Jun 12-14 1985, Cambridge, MA, Engl, p 129-135
- Klink, S.A. "Actual Elastic Modulus of Concrete." ACI Journal, Sept-Oct. 1985. pp 630-633.

- Klink, S.A. "Actual Poisson Ratio of Concrete." *ACI Journal*, November-December 1985. pp 813-817.
- Kraus, D., Roetzer, J., and Thoma, K., "Effect of High Explosive Detonations on Concrete Structures," *Nuclear Engineering and Design*, Vol. 150, No. 2-3. 1994, pp 309-314.
- Krauthammer, T. and R. K. Otani, "Mesh, Gravity and Load Effects on Finite Element Simulations of Blast Loaded Reinforced Concrete Structures," *Computers and Structures*, v 63, n 6, Jun, 1997, p 1113-1120
- Krauthammer, T. and R. K. Otani, "Assessment of Reinforced Details for Blast Containment Structures," *ACI Structural Journal*, v 94, n 2, Mar-Apr, 1997, p 124-132
- Krauthammer, T., Marchand, K. A., Stevens, D. J., Bounds, W. L., and Nene, M., "Effects of Short Duration Dynamic Loads on RC Structures," *Concrete International*, Vol. 16, No. 10, 1994, pp. 57-63.
- Lok, T. S., and Xiao, J. R., "Steel-Fibre-Reinforced Concrete Panels Exposed to Air Blast Loading," *Proceedings of the Institution of Civil Engineers, Structures and Buildings*, Vol. 134, No. 4, 1999, pp. 319-331.
- Lawrence Livermore National Laboratory (1999). "DYNA3D A nonlinear, explicit, three-dimensional finite element code for solid and structural mechanics-user manual."
- Lew, H.S. and Reichard, T.W. "Mechanical Properties of Concrete at Early Ages." *ACI Journal*. October 1978, pp 533-542.
- Longinow, A., and Mniszewski, K.R., "Protecting Buildings Against Vehicle Bomb Attacks," *Practice Periodical on Structural Design and Construction*, Vol. 1, No. 1, 1996, pp. 51-54.
- Low, H.Y and Hong, H. "Reliability analysis of direct shear and flexural failure modes of RC under explosive loading." *Engineering Structures*, v24, n2, February 2002, pp 189-198.

- Low, H.Y. "Reliability analysis of reinforced concrete slabs under explosive loading." *Structural Safety*, v23, n2, 2001, pp 157-178.
- Mays, G.C., Hetherington, J.G., and Rose, T.A. "Response to Blast Loading of Concrete Wall Panels with Openings," *ASCE Journal of Structural Engineering*, Vol. 125, No. 12. 1999, pp. 1448-1450.
- Mirza, S.A., Hatzinikolas, M, and MacGregor, J.G. "Statistical Descriptions of Strength of Concrete." *ASCE Journal of the Structural Division*, Vol. 105, No. ST6, June 1979. pp 1021-1035.
- Melchers, R.E. "Structural Reliability: Analysis and Prediction," 2<sup>nd</sup> Ed. John Wiley & Sons, Ltd. New York, 2002.
- Murray, Y.D. (1997). "Composite retrofit techniques for blast resistance, Rep. DSWA-TR-97-00." Defense Threat Reduction Agency, Dulles, VA.
- National Concrete Masonry Association (1994). "Research Evaluation of the Flexural Tensile Strength of Concrete Masonry, Project # 93-172."
- Nowak, A.S. and Collins, K.R. "Reliability of Structures." McGraw Hill, 2000.
- Otani, R. and Krauthammer, T. "Assessment of Reinforcement Details for Blast Containment Structures." *ACI Structural Journal*. March-April 1997, pp. 124-132.
- Rabbat, B.G. and Russell, H.G. "Friction coefficient of Steel on Concrete or Grout." *ASCE Journal of Structural Engineering*, v111, n3, March 1985, pp 505-515.
- Rackwitz, R. and Fiessler, B., (1978) "Structural reliability under combined random load sequence," *Computers and Structures*, 9: 484-494
- Rose, T.A., Smith, P.D., and Mays, G.C. "Protection of Structures Against Airblast using

- Barriers of Limited Robustness,” Proceedings of the Institution of Civil Engineers, Structures and Buildings, Vol. 128, No. 2, 1998, pp. 167-176.
- Rose, T.A., Smith, P.D., and Mays, G.C. “Design Charts Relating to Protection of Structures Against Airblast from High Explosives,” Proceedings of the Institution of Civil Engineers, Structures and Buildings, Vol. 122, No. 2, 1997, pp. 186-192.
- Rosenblueth, E. “Two-Point Estimates in Probabilities,” Journal of Applied Mathematical Modeling, May, pp 327-333, 1981.
- Stewart, M.G., Netherton, M.D., and Rosowsky, D.V. “Terrorism Risks and Blast Damage to Built Infrastructure,” ASCE Natural Hazards Review, v7, n3, 2006, pp. 114-122.
- Volkman, Douglas E. “Aspects of Blast Resistant Masonry Design,” ASTM Special Technical Publication, Masonry: Components to Assemblages, Dec 5 1989, 1990, Orlando, FL.
- Widder, J.M. “Review of Methodologies for Assessing the Blunt Trauma Potential of Free Flying Projectiles Used in Non-Lethal Weapons.” Battelle Edgewood Operations, March 2000.
- Zehrt, William H., LaHoud, Paul M., and Bogosian, David D., “Blast Response in Concrete Walls,” *Concrete International*, v 20, n 12, Dec, 1998, p 27-31
- Zehrt, W.H, and LaHoud, P.M. “Development of Design Criteria for Reinforcing Steel Splices in Blast Resistant Concrete Structures,” Concrete and Blast Effects, American Concrete Institute, SP-175, ed. Bounds, W., 1998, pp. 131-140.

## **List of Figures**

**Figure 1. Finite Element Models for Grouted and Ungouted CMU Walls**

**Figure 2. Typical Experimental and Idealized Load Curves**

**Figure 3. Load Curve Random Variables**

**Figure 4. Resistance RV Sensitivity Analysis**

**Figure 5. High, Moderate, and Low Mean Load Curves**

**Figure 6. Probability Density Functions of Load Curve Impulse**

**Figure 7. Cumulative Distribution Functions of Load Curve Impulse**

**Figure 8. Mean Load Curves Resisted for Wall Failure and Critical Debris Velocity**

## **List of Tables**

**Table 1. Random Variables**

**Table 2. Reliability Indices, Wall Failure**

**Table 3. Reliability Indices, Critical Velocity**

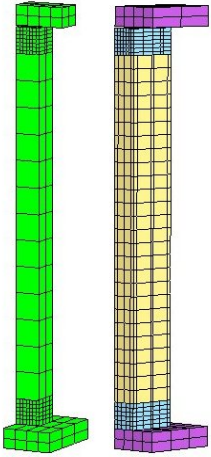


**Figure 1. Finite Element Models for Grouted and Ungouted CMU Walls**

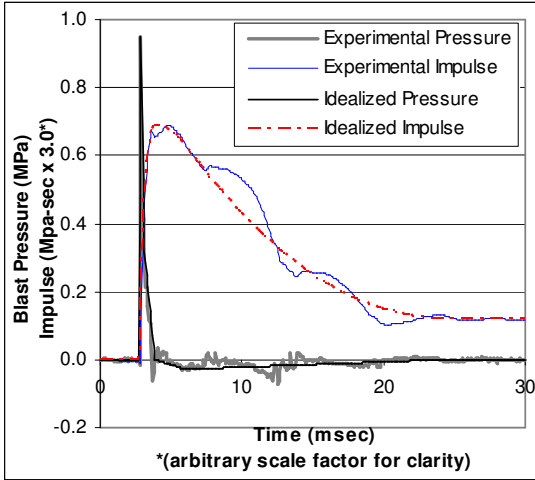


**Figure 2. Typical Experimental and Idealized Load Curves**

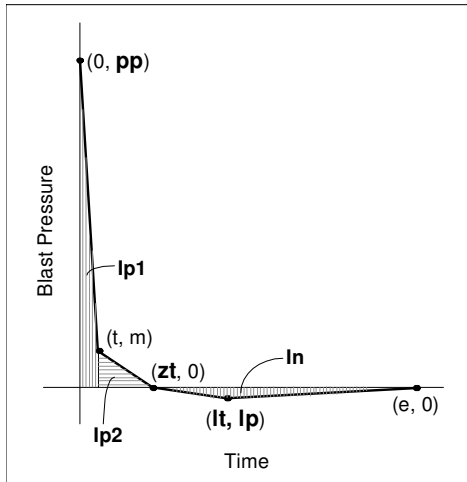


**Figure 3. Load Curve Random Variables.**

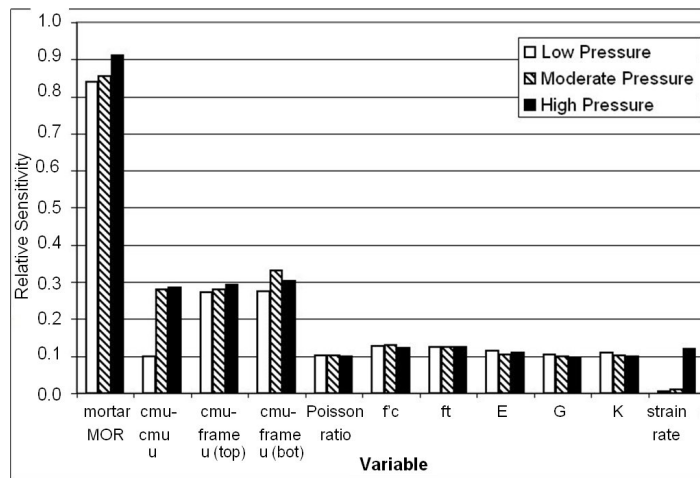


**Figure 4. Normalized Resistance RV Sensitivity Analysis**

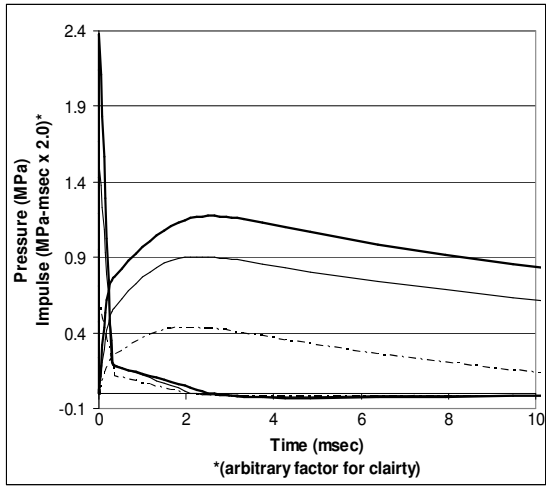


**Figure 5. High, Moderate, and Low Mean Load Curves**

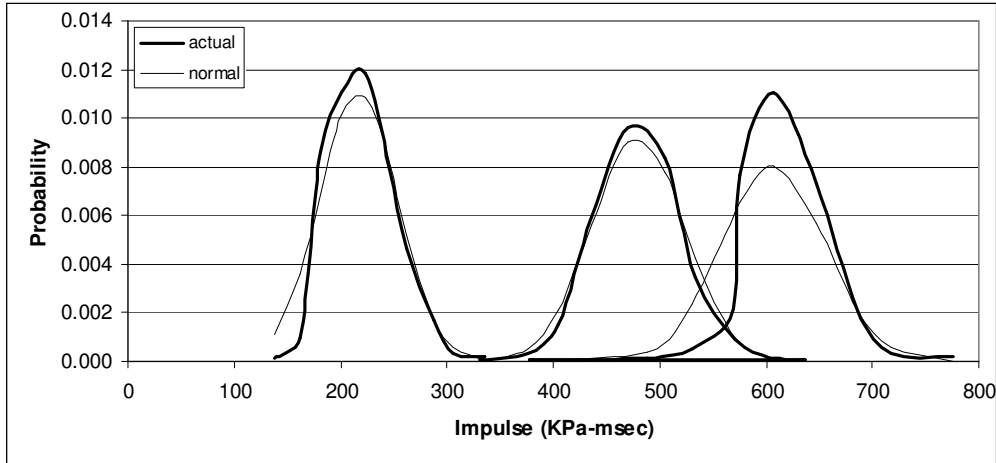


**Figure 6. Probability Density Functions of Load Curve Impulse**

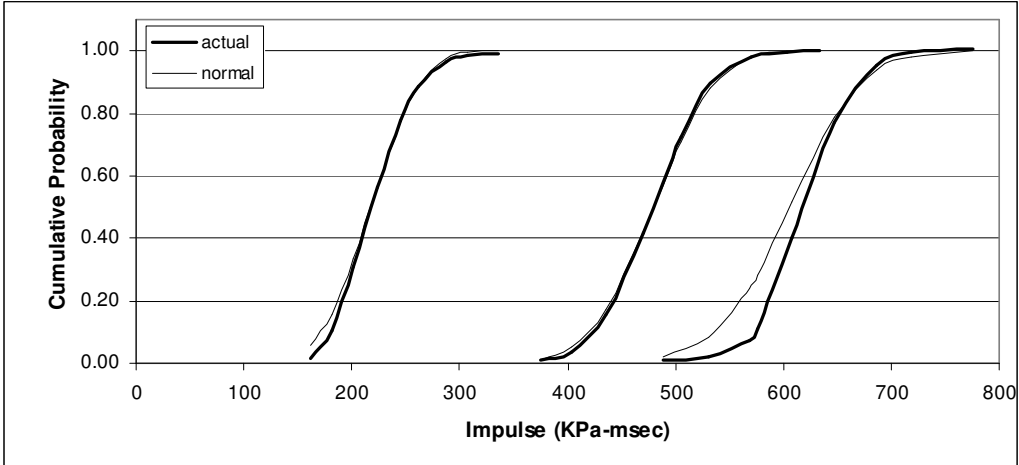


**Figure 7. Cumulative Distribution Functions of Load Curve Impulse**

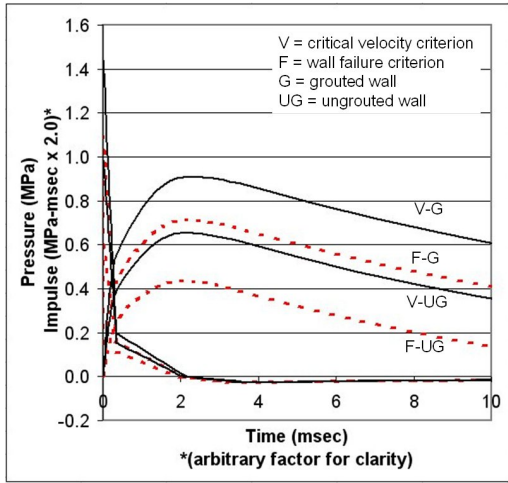


**Figure 8. Mean Pressure and Impulse Load Curves Resisted for Wall Failure and Critical Debris Velocity**

**Table 1: Random Variables**

Random Variable	Low Pressure		Moderate Pres.		High Pressure	
	mean	COV	mean	COV	mean	COV
Primary positive impulse (Ip1)	82.8	0.25	219	0.18	325	0.14
Secondary positive impulse (Ip2)	133	0.17	257	0.24	283	0.25
Negative Impulse (In)	209	0.14	249	0.18	238	0.25
Zero pressure time (zt)	1.97	0.20	2.16	0.13	2.45	0.11
Peak pressure (pp)	587	0.17	1518	0.24	2381	0.25
Low pressure (lp)	-24.9	0.14	-25.3	0.18	-30.8	0.25
Low pressure time (lt)	3.31	0.20	3.73	0.13	4.26	0.11

Units: time=ms, pressure=KPa

**Table 2: Load Random Variable Correlations**

Low Pressure		Moderate Pres.		High Pressure	
RVs	$\rho$	RVs	$\rho$	RVs	$\rho$
pp, Ip2	1	pp, Ip2	1	pp, Ip2	1
lp, In	1	lp, In	1	lp, In	1
lt, zt	1	lt, zt	1	lt, zt	1
In, Ip2	0.30	In, Ip2	0.25	In, Ip2	-0.20
Ip1, In	0.47	Ip1, Ip2	-0.75	Ip1, Ip2	-0.80
				zt, Ip2	0.73

**Table 3. Resistance Random Variables**

Random Variable	mean	COV
Mortar Joint Strength (mj1 – mj15)	1.73	0.24
Block-Block Joint Friction (uj1 – uj14)	0.50	0.11
Upper Block-Frame Friction (ut)	0.65	0.11
Lower Block-Frame Friction (ub)	0.65	0.11

\*Units: stress = MPa

**Table 4. Reliability Indices, Wall Failure**

Pe	Blast Pressure	Fully-Grouted Walls			Ungouted Walls		
		Normal	Lognorm	Ext I	Normal	Lognorm	Ext I
1.0	Low	1.92	<b>1.89</b>	1.91	0.07	<b>0.09</b>	0.14
	Moderate	<b>-1.55</b>	-1.59	-1.59	<b>-4.08</b>	-4.32	-4.70
	High	-3.07	-3.18	<b>-3.34</b>	-5.75	-6.24	<b>-7.07</b>
0.10	Low	2.78	<b>2.75</b>	2.77	1.67	<b>1.68</b>	1.70
	Moderate	<b>1.32</b>	1.31	1.31	<b>1.28</b>	1.28	1.28
	High	1.28	1.28	<b>1.28</b>	1.28	1.28	<b>1.28</b>
0.01	Low	3.46	<b>3.44</b>	3.45	2.60	<b>2.60</b>	2.62
	Moderate	<b>2.35</b>	2.35	2.35	<b>2.33</b>	2.33	2.33
	High	2.33	2.33	<b>2.33</b>	2.33	2.33	<b>2.33</b>
0.001	Low	4.03	<b>4.02</b>	4.03	3.31	<b>3.31</b>	3.32
	Moderate	<b>3.11</b>	3.11	3.11	<b>3.09</b>	3.09	3.09
	High	3.09	3.09	<b>3.09</b>	3.09	3.09	<b>3.09</b>
0.0001	Low	4.55	<b>4.53</b>	4.54	3.90	<b>3.91</b>	3.92
	Moderate	<b>3.73</b>	3.73	3.73	<b>3.72</b>	3.72	3.72
	High	3.72	3.72	<b>3.72</b>	3.72	3.72	<b>3.72</b>

**Table 5. Reliability Indices, Critical Velocity**

Pe	Blast Pressure	Fully-Grouted Walls			Ungouted Walls		
		Normal	Lognorm	Ext I	Normal	Lognorm	Ext I
1.0	Low	4.19	<b>3.79</b>	3.35	2.15	<b>2.07</b>	2.01
	Moderate	<b>-0.39</b>	-0.36	-0.30	<b>-2.69</b>	-2.80	-3.10
	High	-2.34	-2.40	<b>-2.61</b>	-4.61	-5.01	<b>-5.95</b>
0.10	Low	4.69	<b>4.33</b>	3.94	2.95	<b>2.89</b>	2.84
	Moderate	<b>1.51</b>	1.52	1.54	<b>1.28</b>	1.28	1.28
	High	1.29	1.29	<b>1.28</b>	1.28	1.28	<b>1.28</b>
0.01	Low	5.14	<b>4.81</b>	4.46	3.60	<b>3.55</b>	3.51
	Moderate	<b>2.48</b>	2.49	2.50	<b>2.33</b>	2.33	2.33
	High	2.33	2.33	<b>2.33</b>	2.33	2.33	<b>2.33</b>
0.001	Low	5.55	<b>5.25</b>	4.93	4.16	<b>4.12</b>	4.08
	Moderate	<b>3.22</b>	3.22	3.23	<b>3.09</b>	3.09	3.09
	High	3.09	3.09	<b>3.09</b>	3.09	3.09	<b>3.09</b>
0.0001	Low	5.94	<b>5.66</b>	5.37	4.66	<b>4.62</b>	4.59
	Moderate	<b>3.83</b>	3.83	3.84	<b>3.72</b>	3.72	3.72
	High	3.72	3.72	<b>3.72</b>	3.72	3.72	<b>3.72</b>